

Design and analysis of concave diffraction grating with one-dimensional photonic bandgap structure

Yuzheng Mao^{1,2} · Jingping Zhu^{1,2} · Bingzheng Du^{1,2} · Xun Hou^{1,2}

Received: 19 March 2017/Accepted: 7 July 2017/Published online: 12 July 2017 © Springer Science+Business Media, LLC 2017

Abstract Matching one-dimensional photonic bandgap theory with the grating condition, a novel design approach of the etched diffraction grating for the demultiplexer was proposed. With a stack of eight alternating dielectric layers per grating tooth, a computed reflection efficiency of 98% around the central wavelength was achieved by this method. The grating efficiency approached -0.78 dB with a channel uniformity of 0.06 dB over 120 nm bandwidth, and the neighbor channel crosstalk was better than -20 dB. An analysis of etching deviation suggests that the diffraction grating designed by this approach is very tolerant concerning fabrication imperfections.

Keywords Diffraction grating · One-dimensional photonic crystal · Wavelength division multiplexer · Reflection bandgap · Plannar waveguide

1 Introduction

The increasing demand for data transmission has contributed to the development of wavelength division multiplexing (WDM) communication system. Optical demultiplexers are essential components of the system, which can significantly enhance the optical fiber capacity (Fujii and Minowa 1983). Among various technologies available for implementing (de)multiplexer functionality, planar integrated devices have drawn much attention owning to their compactness, better stability, and lower cost (He et al. 1998). The two main techniques commonly used are the array waveguide grating (AWG) and the concave diffraction

Shaanxi Key Lab of Information Photonic Technique, Xi'an Jiaotong University, Xi'an 710049, China



[☑] Jingping Zhu jpzhu@xjtu.edu.cn

Key Laboratory for Physical Electronics and Devices of the Ministry of Education, Xi'an Jiaotong University, Xi'an 710049, China

grating (CDG) (Smit and Van Dam 1996; Janz et al. 2004). AWGs based on silica on silicon with low index contrast material system have been commercially used due to advantages of fabrication tolerance, low propagation losses, and good direct coupling to optical fibers (Fujii and Minowa 1983; He et al. 1998). However, the AWG uses an array of waveguides to define a wavelength-dependent phase distribution, which occupies a relatively large area on the chip. Crosstalk may also occur owning to phase errors, and it also has a poor thermal stability. Furthermore, the efficiency of the device is limited due to the mode-field transition loss that occurs at the junction between slab and arrayed waveguides (Okamoto 2014).

Compared to the AWG, the CDG works in reflection mode, and only one laterally free propagation region is required. In addition, by replacing the array of waveguides with the grating teeth to disperse the wavelengths, the size of the grating can be further reduced, which makes it more competitive (Wang et al. 2004; Pathak et al. 2014). Conventional CDGs need a relatively deep etching, so that the performance of the device critically depends on the smoothness and verticality of the grating facets (Jafari and Kirk 2011). Several configurations have been proposed to overcome these constrains, e.g. total internal reflecting (retro-reflecting) facets, and metallized grating facets (Erickson et al. 1997; Pottier and Packirisamy 2012). However, the grating efficiency is limited due to the corner effect in fabrication and absorption. A more promising approach is the use of a Bragg reflector with shallow etching for each facet, which offers advantages of high efficiency, low insertion loss, and simple fabrication process. Much research has been performed on the Bragg-CDG designs. Brouckaert et al. (2007) prepared a four-channel plannar concave grating on SOI platform, and the insertion loss can be reduced down to 1.9 dB by replacing each facet with a second-order distributed Bragg reflector (DBR). However, the DBR grating does not allow for a continuity of Bragg layers between successtive facets, leading to an extra scattering loss when fabricated. Pottier and Packirisamy (2013) proposed an etched grating based on continuous elliptical Bragg facets followed by an odd-order quarter wavelength dielectric reflector with a considerable reflection efficiency. But the Bragg period derived from the diffraction condition can not match with a perfect Bragg reflection condition exactly, as the refractive indices of materials cannot be freely chosen practically, causing a narrow output bandwidth. Moreover, a complicated fabrication process was required, since the Bragg facet consists of twenty periods of alternating dielectric stripe.

It is necessary to attain high reflectance in designing the diffraction grating, and a photonic crystal can be a perfect mirror for light from any direction within a specified frequency range (Winn et al. 1998). Therefore, this paper presents a novel method based on one-dimensional photonic bandgap structure to design the CDG, which makes a good match between the reflection condition and diffraction condition. The reflection condition of the photonic crystal is related to a transfer matrix, so that the appropriate grating parameters can be obtained. Two gratings with different reflection conditions are designed and simulated using a finite-difference time-domain (FDTD) method. In addition, the effect of the etching deviation on the grating efficiency is discussed. Finally, a three-dimensional (3D) simulation of an individual Bragg grating facet is performed. The simulation results and analysis are also presented.

2 Design theory

A one-dimensional photonic crystal (1-D PC) consists of alternating dielectric layers coupled to a homogeneous medium, shown in Fig. 1. d_1 and d_2 are the width of stripes with



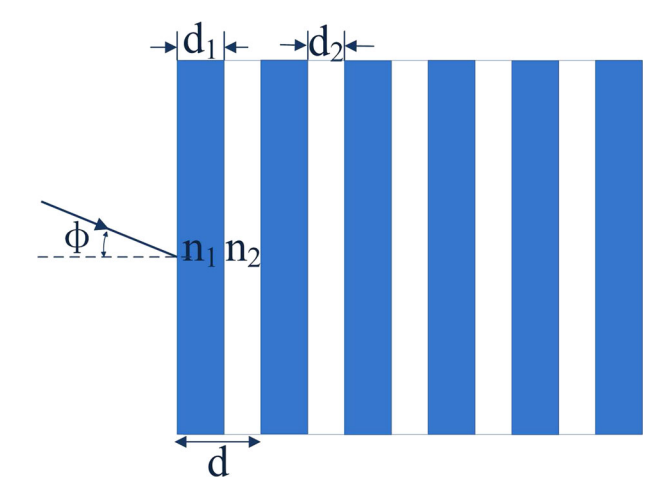


Fig. 1 Schematic of a one-dimensional photonic crystal structure

refractive indices of n_1 and n_2 for the respective layers, which creates a basic period d ($d = d_1 + d_2$) of the photonic crystal.

The 1-D PC structure can reflect a specified range of frequencies incident from a particular angle or angular range effectively, which is the optimum choice of grating tooth. Combining the 1-D PC structure with the Roland configuration, a concave diffraction grating was built as shown in Fig. 2. The input and outputs are placed along a circle of radius R_{rc} (the Roland circle). The grating tooth made of 1-D PC sit on a grating circle with a radius $2R_{rc}$ which is tangent to the Roland circle. This concave grating can both diffract and focus the reflected light into the output waveguides on the Roland circle efficiently.

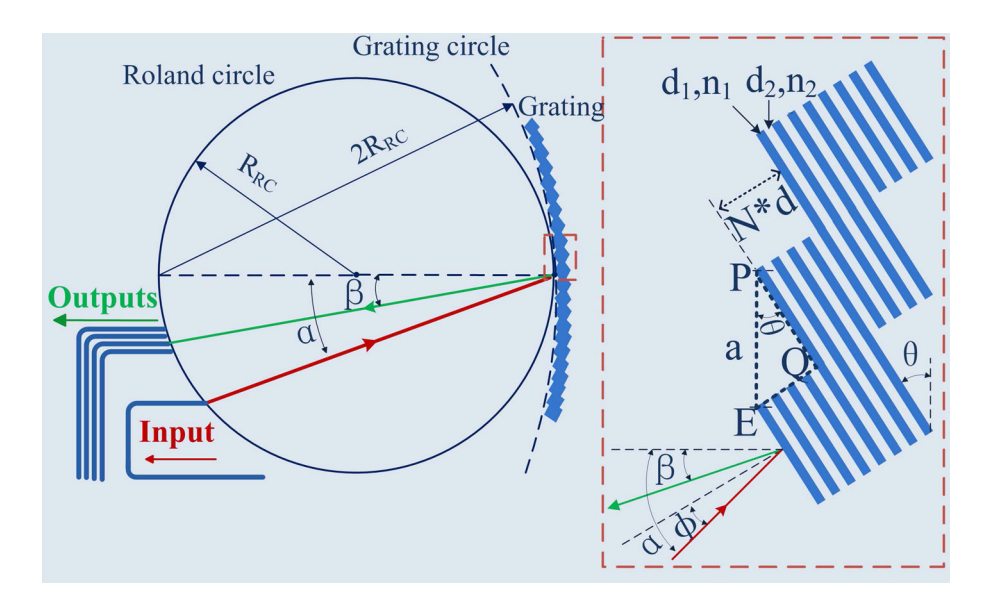


Fig. 2 Schematic layout of a Roland configuration based etched diffraction grating composed of 1-D PC



263 Page 4 of 10 Y. Mao et al.

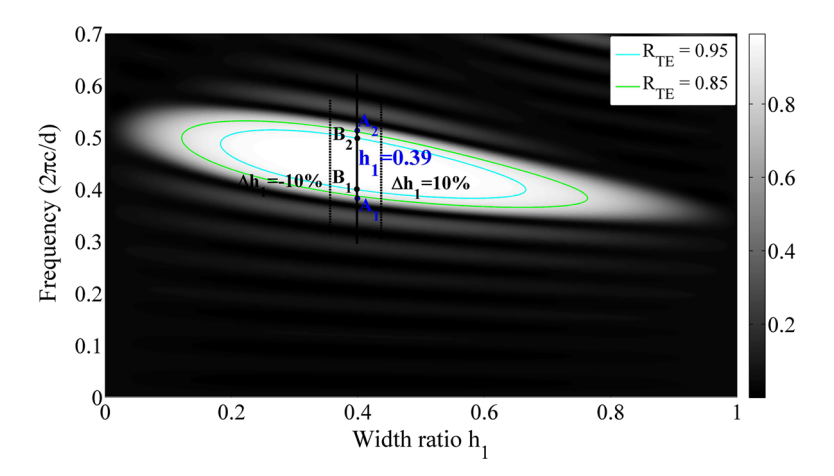


Fig. 3 The reflection band structure of multilayers with $n_1 = 1.44$, $n_2 = 1$, and $\phi = 5^{\circ}$. Propagating states, *black*; evanescent states, *white*

The grating teeth are titled at an angle θ to the grating surface. N is the number of periods per diffraction grating period a. Other parameters, appearing in Fig. 2, are: the incident angle α and the diffracted angle β with respect to the grating normal, the incident angle ϕ on the facet elements.

The propagation characteristics of light waves in the 1-D PC can be related to a unitary 2×2 translation matrix (Fink et al. 1998). The reflection efficiency of the multilayers can be calculated according to the matrix (Born and Wolf 1982). It is convenient to obtain the reflection efficiencies of the infinite structure by projecting the reflectivity formulae onto the ω - h_1 plane. With a particular material system and incident angle ϕ , the reflection band of such structure can be calculated, as shown in Fig. 3. The white areas represent regions with high reflection efficiency, whereas the black areas are regions of propagating states. In Fig. 3, with a selected width ratio h_1 ($h_1 = d_1/d$), the light wave at a frequency $\omega = \varpi \cdot 2\pi c/d$ within high reflection band edges (the respective reflection efficiency are 85% and 95%) will be reflected effectively by the photonic crystal. We define ϖ as the normalized frequency

$$\varpi = \frac{\omega d}{2\pi c} = \frac{d}{\lambda}.\tag{1}$$

For the high reflection band edge from ϖ_1 to ϖ_2 , the respective wavelength ranging from λ_2 to λ_1 can be obtained according to Eq. (1),

$$\lambda_1 = \frac{d}{\varpi_1}, \quad \lambda_2 = \frac{d}{\varpi_2}. \tag{2}$$

To keep an accurate symmetrical reflection spectrum, the central work wavelength of the grating has the form,

$$\lambda_0 = \frac{1}{2}(\lambda_1 + \lambda_2). \tag{3}$$

On substituting Eq. (2) into (3) and solving for d



$$d = \frac{2\lambda_0 \varpi_1 \varpi_2}{\varpi_1 + \varpi_2}. (4)$$

Then the respective dielectric layer thickness d_i can be determined from the equation $d_i = d \times h_i$ (i = 1, 2). With this method, a multilayer grating tooth with high reflection and accurate bandgap can be obtained. For different material systems and incident angles, the design approach can also be used to achieve a large reflection bandwidth by choosing proper width ratio.

For a diffraction grating, the grating condition needs to be fulfilled,

$$M\lambda = na(\sin\alpha + \sin\beta),\tag{5}$$

where M is the diffraction order, n is the effective index of the free propagation region, and a is the grating period. From the grating-stripes geometry (the triangle EPQ), we have

$$\alpha - \theta = \phi \tag{6}$$

$$a = \frac{Nd}{\sin \theta}. (7)$$

Equation (5) then reduces to,

$$M = \frac{nN\varpi}{\sin\theta}(\sin\alpha + \sin\beta). \tag{8}$$

With M an integer, the light with frequency ϖ in the high reflection band will be diffracted efficiently. Setting n_1 , n_2 , ϕ , h_1 , α and λ_0 as the design parameters, d is then obtained from Eq. (4), θ from (6), a from (7), and β from (8).

Up to this point, only the reflection condition is considered. The grating has the maximum efficiency in the given order when it has the identical output angle, i.e., the blazing condition,

$$\alpha - \beta = 2\phi. \tag{9}$$

Using this criterion, Eq. (8) then takes the form,

$$M = 2nN\varpi\cos\phi. \tag{10}$$

This restricts somehow the freedom, as the refractive index n and frequency ϖ cannot be freely chosen because M can only be an integer. However, as shown in the following section, with a small incident angle, good performance can be obtained even away from the blazing condition.

3 Simulation and analysis

Using the theory presented in the preceding section, two concave diffraction gratings with different reflection conditions were designed. The common parameters are $n_1 = 1.44(\text{SiO}_2)$, $n_2 = 1$ (air), $\phi = -5^\circ$, $\lambda_0 = 1.55 \, \mu \text{m}$, and each facet comprises eight periods. The photonic bandgap of the grating facet for TE mode was calculated by the translation matrix method as shown in Fig. 2.



263 Page 6 of 10 Y. Mao et al.

	C 1		C		0 1		
Grating	h_1	ϖ_1	ϖ_2	d (nm)	N	θ (°)	a (nm)
A	0.39	0.376	0.481	654.2	1	35	1140.6
В	0.39	0.389	0.468	658.5	1	35	1148.1

Table 1 Configuration parameters of Grating A and B based on the 1-D PC bandgap theory

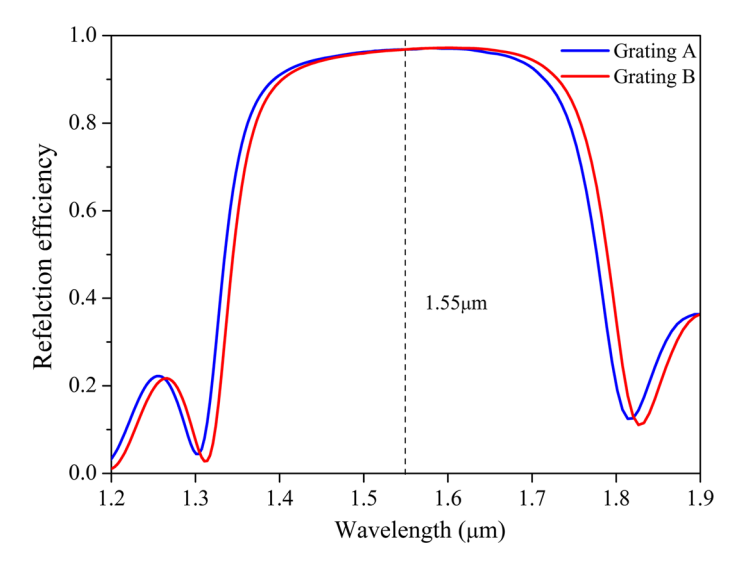


Fig. 4 The reflection spectra of an individual facet of Grating A and B

3.1 Comparision of two gratings

With $h_1 = 0.39$, we choose reflection efficiencies of 85% (Point A_1 and A_2) and 95% (Point B_1 and B_2) as the bandgap edge to design Grating A and B, respectively. d can be calculated according to Eq. (4). The parameters of Grating A and B are listed in Tabel 1. With the incident angle $\alpha = 30^{\circ}$ and $R_{rc} = 400 \, \mu m$, the simulations were performed using FDTD Solutions software in a two-dimensional way. The reflection spectra of two gratings were calculated in Fig. 4. Note that both Grating A and B have large reflection bandwidths and efficiencies up to 98% around the central wavelength. The reflection efficiency will further increase with the number of dielectric layers each grating facet. Moreover, the reflection band of Grating B exhibits a red shift compared to that of Grating A, which can be deduced from Eq. (2). For a given width ratio, the respective ϖ is constant (solid vertical line in Fig. 3) so that the light wavelength increases with the period d.

The computed efficiencies of Grating A and B are displayed in Figs. 5 and 6, respectively, which corresponds to the grating efficiency for the diffracted order. For Grating A, the diffraction efficiency is about -0.78 dB, and the next-channel crosstalk is -20.7 dB. The channel uniformity is 0.06 dB over the 120 nm spectral range. For Grating B, the diffraction efficiency is about -0.79 dB, and the next-channel cross talk is -20.9 dB. The channel uniformity is 0.09 dB over the 120 nm spectral range. It shows that Grating A and B have high diffraction efficiencies and low next-channel crosstalk with similar level,



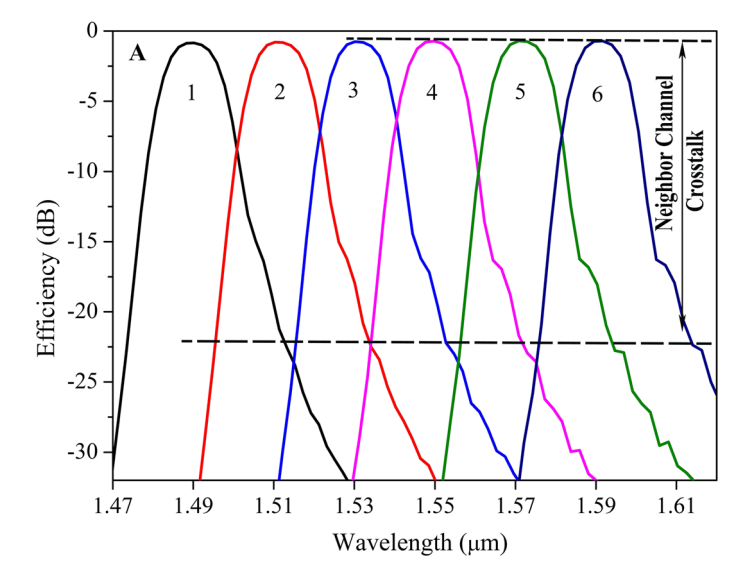


Fig. 5 Output spectra efficiencies of Bragg Grating A with the numbered channels

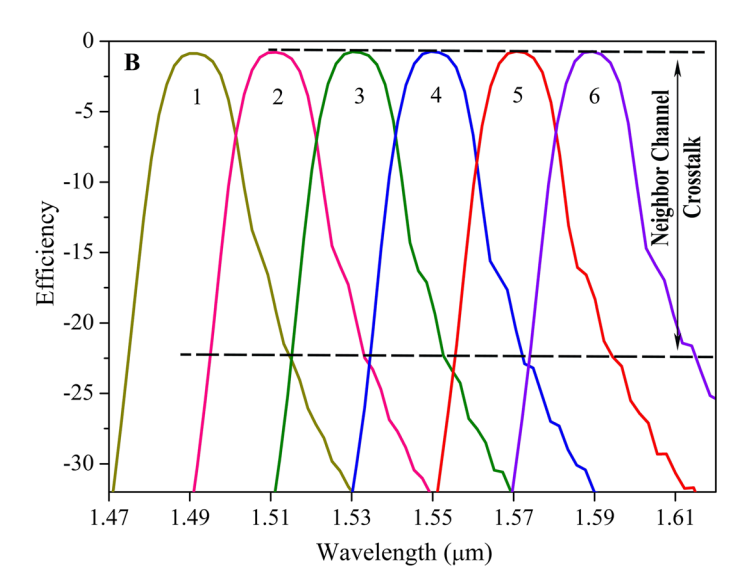


Fig. 6 Output spectra efficiencies of Grating B with the numbered channels

which indicates that both gratings can be used for the demultiplexer. In addition, Grating A performs slightly better than Grating B in the channel uniformity due to the fact that Grating A has a flatter reflection band from 1.49 to 1.59 μm (see Fig. 4).

The spatial distributions of light of two gratings for TE mode with four channels in a 20 nm channel spacing are presented in Fig. 7. It can be observed that different light waves get diffracted into different directions with a considerable linear dispersion, and the



263 Page 8 of 10 Y. Mao et al.

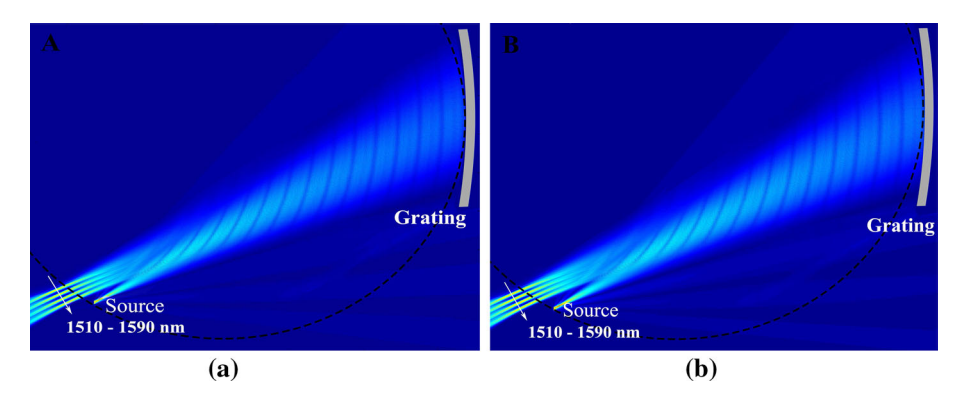


Fig. 7 Spatial distribution of light of the CDG from 1510 to 1590 nm with a channel spacing of 20 nm, Grating A (a), and Grating B (b)

diffraction angle has a slight difference owning to the difference of the grating period between Grating A and B.

Moreover, for the two gratings, almost all the light gets diffracted into an order of M=1 and the other diffraction orders are suppressed. As a result, both gratings exhibit high diffraction efficiencies at the expected directions.

In summary, both Grating A and B behave well in terms of efficiency, crosstalk and channel uniformity. This suggests the performance of grating designed by 1-D PC bandgap theory is insensitive to changes in grating parameters, which results in a good tolerance on fabrication errors for the grating. A further research was carried out to support it.

3.2 Etching deviation analysis

For Grating A, with d constant, the deviation of the width ratio varies from -10 to 10% (corresponding to the etching deviation of the layers). Figure 8 presents the reflection spectra of gratings for different cases. The reflection bands are red-shifted when the deviation of h_1 is from -10 to 10%. However, the entire 1.45-1.63 μ m wavelength range keeps a high reflection efficiency more than 96%, and all the gratings have almost the same output spectra around the central wavelength (see Fig. 8), i.e., a 20% deviation does not lead to a significant decrease in reflection and diffraction efficiencies for wavelengths from 1.49 to 1.59 μ m. An illustration of the result is shown in Fig. 2. The high reflection band edge (ϖ) drops slightly as Δh_1 varies from -10 to 10%, and the wavelength is negatively correlated with the normalized frequency as d keeps constant (Eq. 2). Moreover, the grating period a is constant (Eq. 7), and reflection bands from 1.45 to 1.63 μ m remain unchanged. As a result, the deviation of width ratio has little effect on the output spectrum .

3.3 3D simulation

To estimate the scatting loss of the grating in the third dimension, a three-deimensional (3D) FDTD simulation was also performed. Due to the computation limitation, the reflection of an individual facet of Grating A at the central wavelength of 1.55 μ m was calculated. The facet consists of a waveguide core of thickness d_{core} , surrounded by a cladding of n_{clad} . The index of the core layer was chosen itself so that the effective index of the core keeps constant ($n_{eff} = 1.44$) with a air cladding ($n_{clad} = 1$), which corresponds to



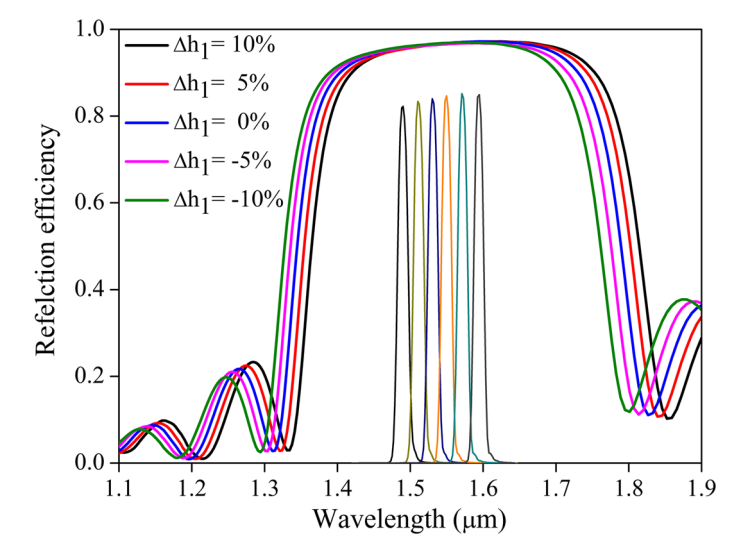


Fig. 8 The reflection spectra for diffraction gratings with a variation of width ratio from -10 to 10% (*thick color lines*), the output through different channels from 1.49 to $1.59\,\mu m$ (*thin color lines*). (Color figure online)

the configuration (Fig. 3). The reflection efficiency of the grating facet with different core thickness was simulated, as shown in Fig. 9. Note that the reflection efficiency increases with the etching depth, and it can be up to 92.5% even if the core thickness is reduced down to $0.5 \ \mu m$. This suggests that the configuration has an extremely low scatting loss and could be employed to realize the demultiplexer.

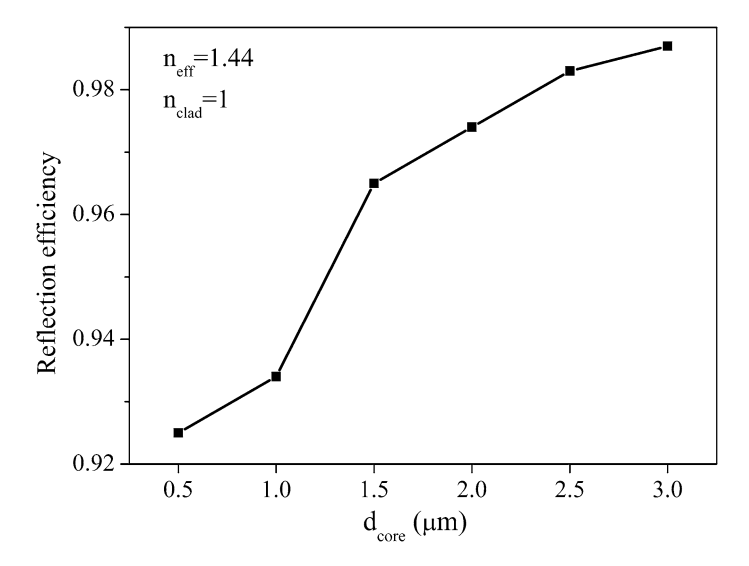


Fig. 9 The reflection efficiency of the Bragg facet calculated by a 3D FDTD simulation when the core thickness was from 0.5 to 3 μ m ($n_{eff}=1.44$ and $n_{clad}=1$)



263 Page 10 of 10 Y. Mao et al.

4 Conclusion

We combine 1-D photonic crystal bandgap structure with Roland configurations to design the EDGs. With this method, two gratings with different parameters were designed and simulated. The results showed that both gratings provide high reflection efficiencies up to 98% with a large bandwidth, and the on-chip loss was reduced down to 0.78 dB with greater channel uniformity. Moreover, this method is very tolerant concerning parameters selection and fabrication imperfections. Such devices can be integrated on a chip to realize the demultiplexer and microspectrometer.

Acknowledgements This work was supported by the Key Research and Development Plan Foundation of Jiangsu Province, China (Grant No. BE2016133).

References

- Born, M., Wolf, E.: Principles of Optics, pp. 55-68. Pergamon Press, Oxford (1982)
- Brouckaert, J., Bogaerts, W., Dumon, P., Schrauwen, J.: Planar concave grating demultiplexer on a nanophotonic silicon oinsulator platform. J. Lightw. Technol. 25, 1269–1275 (2007)
- Erickson, L., Lamontagne, B., He, J.J., Delage, A.: Using a retro-reflecting echelle grating to improve WDM demux efficiency. In: Proceedings of 1997 Digest of the IEEE/LEOS Summer Topical Meetings, pp. 82–83. Montreal (1997)
- Fink, Y., Winn, J.N., Fan, S., et al.: A dielectric omnidirectional reflector. Science 282, 1679–1682 (1998)
 Fujii, Y., Minowa, J.: Optical demultiplexer using a silicon concave diffraction grating. Appl. Opt. 22, 974–978 (1983)
- He, J.J., Lamontagne, B., Ge, A., Erickson, L., Davies, M., Koteles, E.S.: Monolithic integrated wavelength demultiplexer based on a waveguide rowland circle grating in InGaAsP/InP. J. Lightw. Technol. 16, 631–638 (1998)
- Jafari, A., Kirk, A.G.: Demonstration of distributed etched diffraction grating demultiplexer. IEEE Photon. J. 3, 651–657 (2011)
- Janz, S., Balakrishnan, A., Charbonneau, S., Cheben, P.: Planar waveguide echelle gratings in silica-onsilicon. IEEE Photon. Technol. Lett. 16, 503-505 (2004)
- Okamoto, K.: Wavelength-division-multiplexing devices in thin SOI: advances and prospects. IEEE J. Sel. Top. Quantum Electron. **20**, 248–257 (2014)
- Pathak, S., Dumon, P., Van Thourhout, D., Bogaerts, W.: Comparison of AWGs and echelle gratings for wavelength division multiplexing on silicon on insulator. IEEE Photon. J. 6, 1–9 (2014)
- Pottier, P., Packirisamy, M.: High efficiency metallic multistratum concave diffraction grating. Appl. Opt. 51, 4073–4077 (2012)
- Pottier, P., Packirisamy, M.: Design and properties of concave diffraction gratings based on elliptical bragg mirrors. J. Lightw. Technol. 31, 1890–1898 (2013)
- Smit, M.K., Van Dam, C.: Phasar-based WDM-devices: principles, design and applications. IEEE J. Sel. Top. Quantum Electron. 2, 236–250 (1996)
- Wang, W., Tang, Y., Wang, Y., Qu, H., et al.: Etched diffraction grating based planar waveguide demultiplexer on silicon on insulator. Opt. Quantum Electron. 36, 559–566 (2004)
- Winn, J.N., Fink, Y., Fan, S., Joannopoulos, J.D.: Omnidirectional reflection from a one-dimensional photonic crystal. Opt. Lett. 23, 1573–1575 (1998)

